ACS APPLIED MATERIALS & INTERFACES

Research Article

www.acsami.org

Controllable Morphology and Conductivity of Electrodeposited Cu_2O Thin Film: Effect of Surfactants

Ying Yang,*[,†,‡] Juan Han,[†] Xiaohui Ning,[†] Wei Cao,[†] Wei Xu,*[,§] and Liejin Guo[‡]

[†]Shaanxi Provincial Key Laboratory of Electroanalytical Chemistry, Institute of Analytical Science, Northwest University, Xi'an, Shaanxi 710069, People's Republic of China

[‡]International Research Center for Renewable Energy, State Key Laboratory of Multiphase Flow in Power Engineering, Xi'an Jiaotong University, Xi'an, Shaanxi 710049, People's Republic of China

[§]Department of Mechanical Engineering, Stevens Institute of Technology, Hoboken, New Jersey 07030, United States

Supporting Information

ABSTRACT: Both the morphology and conductivity of Cu_2O films are controlled in a facile electrodeposition process by tuning the concentration of surfactants. With the increase of the concentration of sodium dodecyl sulfate (SDS) in the plating solution, the average size of Cu_2O crystals increases, and the electrical conductivity of Cu_2O films changes from n-type to p-type. When the concentrations of SDS are lower than 0.85 mM, the electrodeposited Cu_2O films show n-type conductivity because of the formation of oxygen vacancies or copper atoms. When the concentration of SDS is higher than 1.70 mM, the electrodeposited Cu_2O films show p-type conductivity owing to the formation of copper vacancies. The concentrations of both the donors and the acceptors increase with the concentration of SDS. The effects of surfactants on the morphology and conductivity of electrodeposited Cu_2O films are attributed to the adsorption of SDS molecules on the electrode substrate occupying the deposition sites of Cu^{2+} ions and the adsorption of SDS micelles to Cu^{2+} ions hindering the diffusion of Cu^{2+} ions to the electrode, which affect the reduction rate of Cu^{2+} ions and the formation of oxygen vacancies or copper vacancies during the electrodeposition.

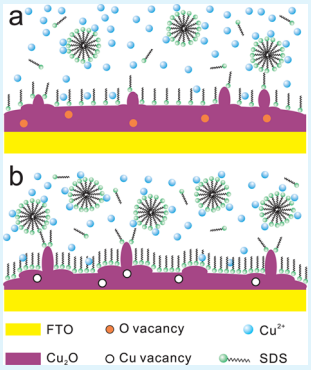

KEYWORDS: *cuprous oxide (Cu_2O), electrodeposition, semiconductor, conductivity, photoelectrochemical cell, surfactant*

1. INTRODUCTION

Cuprous oxide (Cu_2O) has broad applications in photoelectrochemical (PEC) water splitting,[1−4] photocatalysis,[5,6] photovoltaic (PV) cell,[7−10] and PEC CO_2 capture[11−15] due to a direct band gap of approximate 2 eV. Cu_2O generally exhibits as a p-type semiconductor with an acceptor level at 0.45−0.55 eV, which is above the valence band originating from Cu vacancies.[16,17] It can also be tuned to an n-type semiconductor with a donor level at 0.38 eV, which is below the conduction band originating from O vacancies[28] or additional Cu atoms.[18] The tunable conductivity of Cu_2O has attracted a lot of attention for the application in the high-efficiency PV cells based on p-n homojunctions.[19] Researchers have developed various methods to achieve the tunable conductivity of Cu_2O. For example, Wijesundera et al.[18] found that the Cu_2O films behaved as n-type semiconductor when the annealing temperature is lower than 250 °C and as p-type semiconductor when the annealing temperature is higher than 300 °C. The conductivity of Cu_2O also can be tuned by controlling the pH value of plating solutions during electrodeposition. McShane and Choi[20] electrodeposited n-type Cu_2O film in a cupric acetate solution at pH 4.9 and studied the effect of dendritic branching growth of Cu_2O crystals on the photocurrent of films. Tsui and Zangari[21] electrodeposited n-type Cu_2O film on TiO_2 nanotubes in a cupric acetate solution at pH 5.1 to fabricate photoelectrochemical solar cells. Zhao et al.[22] studied the effects of reaction time, deposition potential, and solution temperature on the morphologies of n-type Cu_2O films electrodeposited in an acid cupric acetate solution. On the other hand, Golden et al.[23] and de Jongh et al.[24] electrodeposited p-type Cu_2O films in a cupric sulfate solution at pH 9 on stainless steel and FTO (fluorine doped tin oxide) glass, respectively. Jiang et al.[25] electrodeposited p-type Cu_2O film in a cupric sulfate solution at pH 7−9 and studied the effect of pH value on the carrier concentration of p-type Cu_2O bulk. However, in current methods, the n-type Cu_2O films can only be fabricated in acid plating solutions,[20−22] and the p-type Cu_2O films can only be fabricated in basic solutions.[23−26] It hinders the synthesis of Cu_2O films with p-n homojunctions because a two-step process in two kinds of solutions is required.

In this work, we present a facile method to control both the morphology, mainly about the crystal size, and conductivity (i.e., p-type or n-type) of Cu_2O films in an electrodeposition process by tuning the concentration of sodium dodecyl sulfate (SDS), a kind of anionic surfactants,[27,28] in an acidic plating solution. The effects of SDS concentrations from 0 to 3.30 mM

Received: September 28, 2014
Accepted: December 2, 2014
Published: December 2, 2014

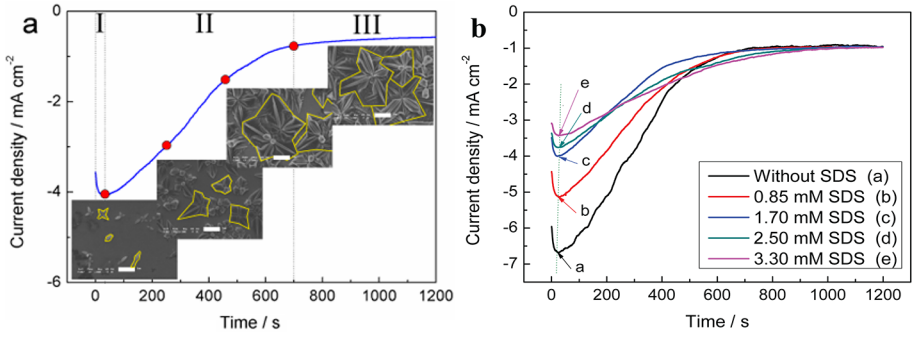

Figure 1. Current density vs deposition time plots of electrochemical deposition of Cu_2O films in cupric acetate solutions (pH 4.93). (a) Illustration of the growth of a Cu_2O film in the plating solution with 1.70 mM SDS (scale bar, 5 μm). (b) Effect of SDS concentrations on deposition current density. The growth of Cu_2O films in the plating solutions with various SDS concentrations is shown in Figure S2 (Supporting Information).

on the morphology and electrical conductivity of electrodeposited Cu_2O have been experimentally investigated. With the increase of the SDS concentration in the plating solution, the average size of Cu_2O crystals increases, and the electrical conductivity of Cu_2O films changes from n-type to p-type. The tunable conductivity is attributed to the adsorption of SDS molecules on the surface of conductive substrate and the adsorption of Cu^{2+} ions on the SDS micelles, which affect the reduction rates of Cu^{2+} ions in the plating solutions and consequently result in the formation of O or Cu vacancies and the tunable conductivity of the Cu_2O films. The method shown in this work provides an effective approach to control the electrical conductivity of Cu_2O thin films for their application in homojunction PV cells.

2. EXPERIMENTAL SECTION

2.1. Fabrication of Cu_2O Films. The electrochemical deposition of Cu_2O films was carried out in a plating solution consisting of 0.05 M cupric acetate. The pH of the solution was adjusted to 4.93[20] by adding a certain amount of acetic acid. To study the effect of surfactants on the properties of Cu_2O films, SDS was added to the plating solution with different concentrations of 0.75−3.30 mM. All the reagents are analytical grade and purchased from the Sinopharm Chemical Reagent Co., Ltd. During the electrodeposition, the plating solution was not stirred, and the solution temperature was kept at 60 °C in a water bath. FTO glass served as the substrate (i.e., working electrode), and a platinum sheet (surface area, 8 cm^2) was used as the counter electrode. A Ag/AgCl (saturated KCl) electrode (+0.222 V vs normal hydrogen electrode, NHE) with a bridging solution of saturated KCl served as the reference electrode, against which all the potentials reported herein were measured. The electrodeposition was operated at −0.1 V for 20 min with a PAR 283 potentiostat (EG&G).

2.2. Morphology and Composition Characterizations. A JSM-6700F field emission scanning electron microscope (FE-SEM, JEOL) and a SSX-550 scanning electron microscope (SHIMADZU) were used to characterize the morphology of Cu_2O films. The X-ray diffraction (XRD) analyses were performed using an X'pert PRO diffractometer (PANalytical) with Cu Kα irradiation (λ = 0.154184 nm) in order to verify the phase and orientation of the deposited films. The compositions of both the original surface and the bulk of Cu_2O films were analyzed with an AXIS UltraDLD X-ray photoelectron spectroscope (XPS, Kratos Analytical) using a monochromatic Al Ka radiation X-ray source (1486.6 eV). To characterize the oxidation state of Cu in the bulk of Cu_2O films, a 2 × 2 mm original surface was etched with a 3.0 keV argon ion beam. The binding energies were referenced to the C 1s peak at 284.8 eV.

2.3. Semiconductor Property Measurements. The band gaps of Cu_2O films were calculated from the optical absorbance in a wavelength range of 300−800 nm by using a U-4100 UV−vis spectrophotometer (Hitachi). The electrical conductivity (n-type or p-type) and the flat band potential of Cu_2O films in a 3 wt % NaCl solution were calculated from the Mott−Schottky measurements using a PAR 283 potentiostat (EG&G) coupled with a Model 5210 lock-in amplifier (EG&G). The data acquisition frequency in the Mott−Schottky measurements was 1000 Hz.

2.4. PEC Characterizations. The PEC experiments were carried out in a 3 wt % NaCl solution under AM 1.5G (100 mW cm^{-2}) simulated illumination provided by a 500 W xenon lamp. A PAR 283 potentiostat (EG&G) was used to measure the photocurrent. A three-electrode setup was used with the Cu_2O film electrode served as the working electrode (illuminating area, 0.785 cm^2), a platinum sheet (surface area, 8 cm^2) as the counter electrode and an Ag/AgCl electrode (saturated KCl) as the reference electrode. During the PEC measurements, the applied potentials were set at the open circuit potential (OCP, −0.05 V in this work).

3. RESULTS AND DISCUSSION

3.1. Growth of Cu_2O Films. The possible reactions during the reduction of Cu^{2+} in cupric acetate solution are[29]

$$2Cu^{2+} + H_2O + 2e^- \rightarrow Cu_2O + 2H^+$$
$$E^\circ = 0.203V_{NHE} + 0.059\ pH \quad (1)$$

$$Cu^{2+} + 2e^- \rightarrow Cu \quad E^\circ = 0.337V_{NHE} \quad (2)$$

$$Cu_2O + 2e^- + 2H^+ \rightarrow 2Cu + H_2O$$
$$E^\circ = 0.471V_{NHE} - 0.059pH \quad (3)$$

where Cu^{2+}, H_2O, e^-, Cu_2O, H^+, and Cu represent dissolved cupric ions, water, electrons, deposited cuprous oxide, adsorbed protons, and metallic copper, respectively. E° is the standard potential. The pH value of the solution at 60 °C decreased slightly from 4.93 to 4.51 with the increase of SDS concentration from 0 to 3.30 mM and the caused change of potential was around 0.02 V according to eqs 1 and 3. Therefore, the effect of SDS concentration on the change of potential is negligible in this study. In a pH 4.93 solution, the standard potentials for reactions in eqs 1, 2 and 3 are 0.272, 0.115, and −0.042 V, respectively. To deposit Cu_2O following eq 1, the deposition potential should be negative than 0.272 V. To provide required overpotential to deposit Cu_2O on FTO glass (the polarization curves are shown in Figure S1 in Supporting Information), we chose a deposition potential of −0.1 V.[20,30]

Figure 1 shows the change of current density and the morphology of Cu_2O crystals during the deposition process. It exhibits three different stages according to the change of current density. In region I, the negative current density

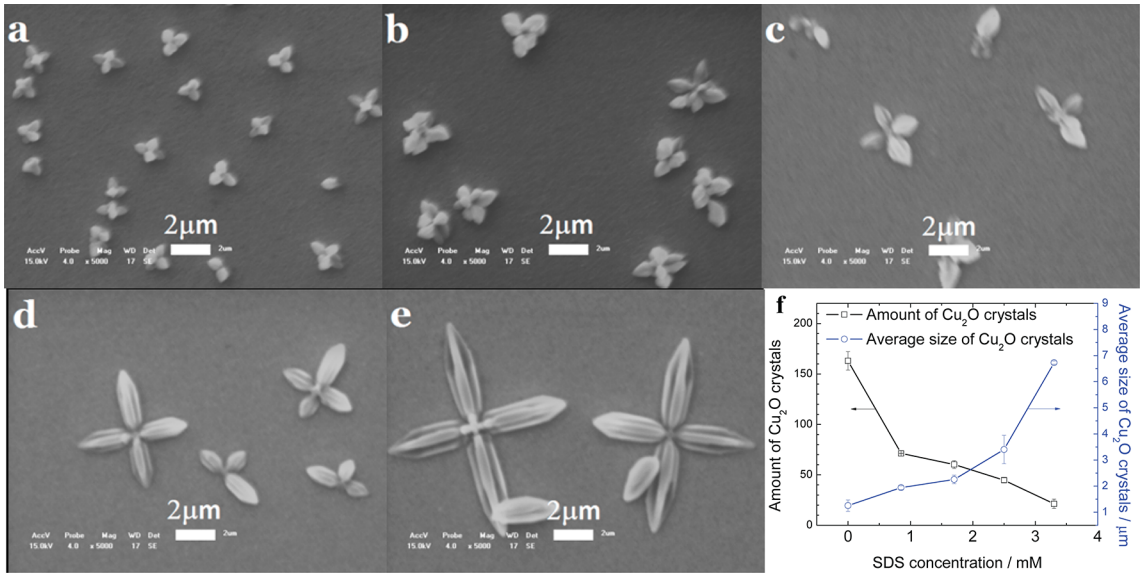

Figure 2. SEM images of Cu_2O microcrystals electrodeposited at the end of region I in cupric acetate solutions (pH 4.93) with (a) 0 M, (b) 0.85 mM, (c) 1.70 mM, (d) 2.50 mM, and (e) 3.30 mM SDS. Scale bars are 2 μm. (f) The amount and the average size of Cu_2O microcrystals under corresponding conditions of panels a−e (observation area, 7271 μm^2).

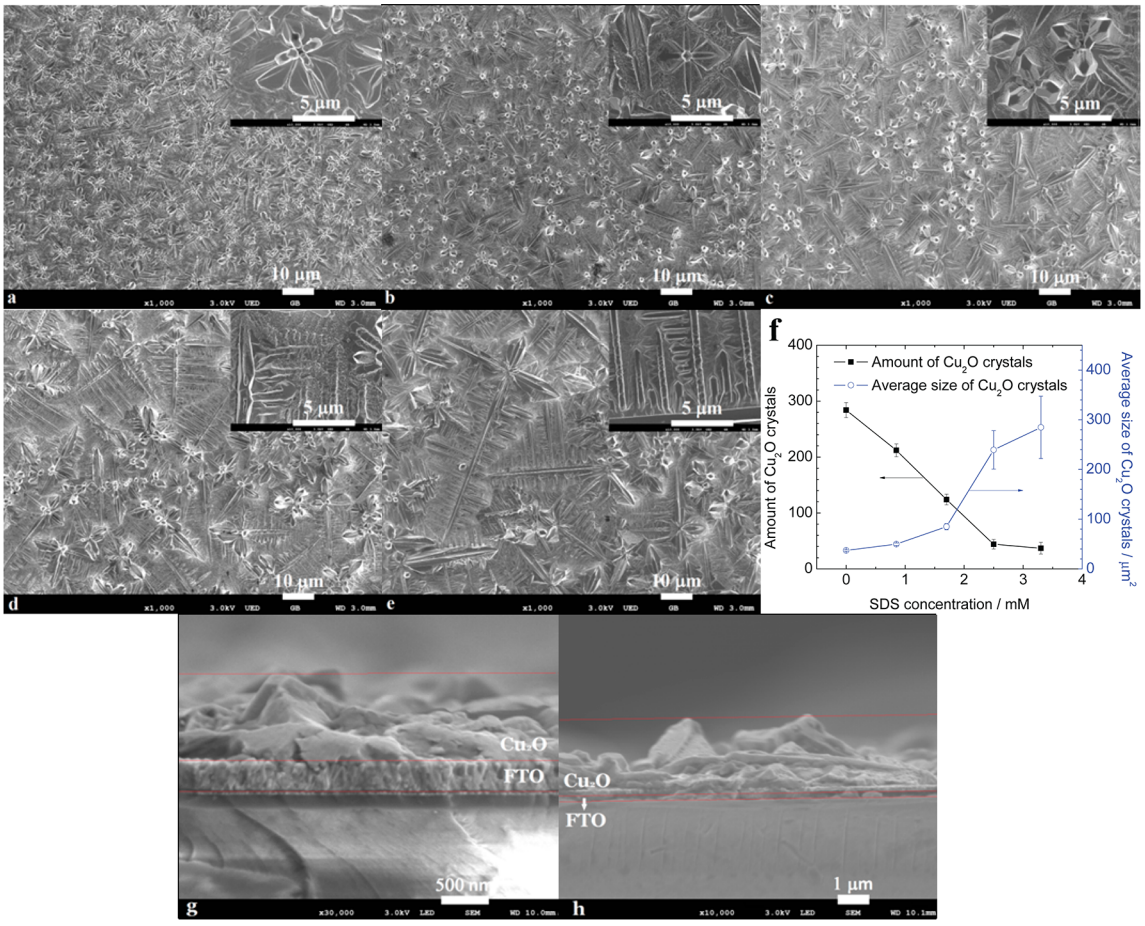

Figure 3. Morphology of Cu_2O thin films electrodeposited on FTO in cupric acetate solutions (pH 4.93) with (a) 0 M, (b) 0.85 mM, (c) 1.70 mM, (d) 2.50 mM, and (e) 3.30 mM SDS, respectively. Scale bars, 10 μm and (insets) 5 μm. (f) The amount and the average size of Cu_2O crystals electrodeposited for 20 min (observation area, 10 535 μm^2). (g) Cross section of sample a (scale bar, 500 nm) and (h) cross section of sample d (scale bar, 1 μm).

decreases sharply to the maximum, which is related with the formation of isolated Cu_2O micron-crystals.[24] The current density then increases gradually in region II with the growth of island-like micron-crystals. Once the edges of micron-crystals

dx.doi.org/10.1021/am506657v | ACS Appl. Mater. Interfaces 2014, 6, 22534−22543

contact each other to form a film covering the entire surface, the increase of current density tends to be moderate, as shown in region III.

The effect of SDS concentration on the current density during the deposition is shown in Figure 1b. Region I (the arrows indicate the nadirs of the curves) becomes longer with the increase of the SDS concentration, which indicates that more time is needed to form Cu_2O micron-crystals. This phenomenon is attributed to the adsorption of SDS molecules on the FTO glass and deposited Cu_2O crystals,[27] which reduces the reduction sites of cupric ions (the electrochemical impedance spectra of FTO glass and Cu_2O film in the water containing different concentrations of SDS have proved this hypothesis and were included in Supporting Information as Figures S3 and S4). Moreover, the reduction current density becomes smaller with the increase of SDS concentration in the plating solution in region I. It suggests the decrease of the amount of Cu_2O micron-crystals formed in region I. This is also confirmed with the morphology of Cu_2O microcrystals at the end of region I, as shown in Figure 2. As the SDS concentration in the plating solutions increases, the amount of Cu_2O micron-crystals decreases and the average size (the length of crystal) increases .

Region II becomes longer with the increase of SDS concentration in the plating solution. It is also attributed to the decreased amount of Cu_2O micron-crystals and increased distance among the Cu_2O crystal islands, so that more time is needed to deposit Cu_2O on the entire FTO surface (Figure S2 in Supporting Information). It should be noted that the slopes of curve of current density vs deposition time in region II (Figure 1b) decrease with the increase of SDS concentration. The result suggests that the growth of Cu_2O crystals becomes slower with the increase of SDS concentration.

At the end of region II, all the edges of crystal islands have contacted and a layer of film formed on FTO substrates. After that (i.e, in region III), the growth of film is predominantly perpendicular to the FTO substrate. In this study, deposition was proceeded for 20 min to ensure the Cu_2O film covering the entire substrate, which is indicated by the plateau shown in the current density vs deposition time plots (Figure 1). The deposited Cu_2O films show orange-red color. Figure 3a–e shows the morphology of Cu_2O films electrodeposited in the plating solutions with 0–3.30 mM SDS for 20 min. It clearly illustrates that the Cu_2O crystals grow uniform. Furthermore, the amount of crystals decreases and the average size of crystals (the crystals are treated as squares, and the average size is the average area of squares) increases with the increase of SDS concentration in the plating solution (observation area, 10 535 μm^2).

The crystals formed on all films show dendritic branching growth because the diffusion of cupric ions in the plating solution cannot replenish the deposition.[20] As can be seen from the insets of Figure 3a–e, the facets of crystal ridges are smooth; however, that of crystal valleys along the substrates are harsh with densely distributed nanopittings. It may result from the nonuniform distribution of cupric ions during the electrodeposition. The ridges can easily contact cupric ions with a higher concentration and grow to perfect facets, while the crystals at the valley form imperfectly due to the shortage of cupric ions. Figure 3g,h shows the cross sections of Cu_2O thin films electrodeposited in cupric acetate solutions without and with 2.50 mM SDS, respectively. The thickness of corresponding Cu_2O thin films are ca. 0.9 and 2.4 μm, respectively. Comparing the thickness of Cu_2O films with the crystal size, it can be seen that the Cu_2O crystals show a lateral preferential growth. This may be attributed to the adsorption of SDS molecules on the crystal facets with high surface energy (such as {100} and {110} facets[31]), leading to the preferential growth of crystal facets with low surface energy (such as {111} facets[31]) along the FTO substrate.

As shown in the aforementioned results, both the deposition rates of Cu_2O (i.e., the reduction rates of Cu^{2+}) and the growth rate of crystals are affected by the concentration of SDS. It is attributed to the adsorption of SDS molecules on the surface of FTO substrate and the adsorption of Cu^{2+} ions on the SDS micelles. In particular, the SDS molecules intend to adsorb on the surface of FTO substrate to reduce the interfacial energy.[27] Therefore, the SDS molecules occupy some reduction sites of cupric ions on the FTO substrate (Scheme 1), which is more

Scheme 1. Growth of Cu_2O Film in Cupric Acetate Solution with SDS.[a]

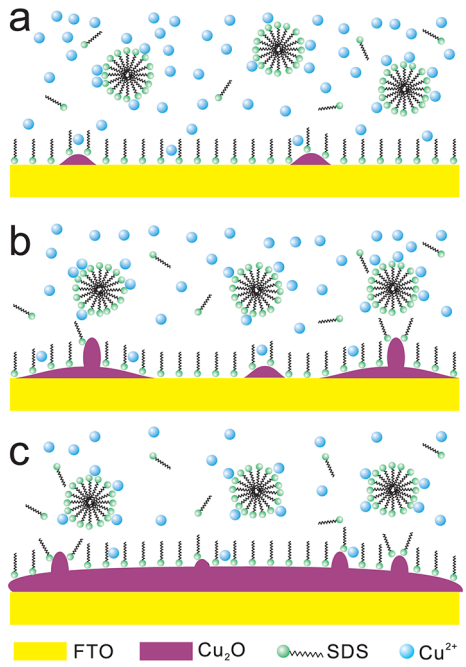

[a]The SDS molecules adsorb on the surface of FTO glass and reduce the contact sites between the cupric ions and the FTO glass. Meanwhile, the SDS micelles adsorb cupric ions in the solution and hinder the diffusion of cupric ions to the interface. (a) The isolated Cu_2O micron-crystals form on the FTO substrate; (b) the micron-crystals grow as islands and cover more area of the FTO substrate; (c) the edges of Cu_2O micron-crystals contact each other and cover the entire surface to form a film.

significant with the increase of the concentration of SDS (Scheme 2). When the SDS concentration is low, more Cu_2O microcrystals are formed at the beginning of electrodepositon because fewer SDS molecules occupy the surface of FTO; with the increase of SDS concentration, the amount of Cu_2O microcrystals formed on the surface decreases because more SDS molecules occupy the surface of FTO (Scheme 2 and Figure 2). Furthermore, the Cu^{2+} ions in the solution were adsorbed on the SDS micelles, which hinders the diffusion of Cu^{2+} ions to the interface.[32] With the increase of SDS concentration in the plating solution, both effects become more significant and further decrease the reduction rate of Cu^{2+} ions

Scheme 2. Mechanism of Controlling Both Morphology and Conductivity of Cu_2O Films by Changing the Concentration of SDS in the Plating Solution during Electrodeposition[a]

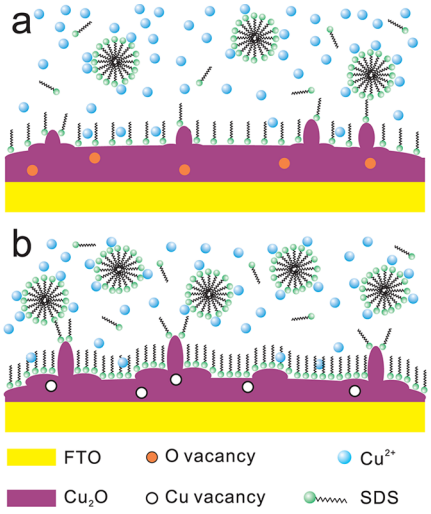

[a]The SDS molecules are adsorbed on the surface of FTO glass and occupy the deposition sites. A higher concentration of SDS results in fewer contact sites. Meanwhile, the SDS micelles adsorb cupric ions in the solution and hinder the diffusion of cupric ions to the interface. With the increase of SDS concentration, the reduction rate of cupric ions becomes smaller. As a consequence, (a) a large amount of small Cu_2O crystals with oxygen vacancies are formed on the substrate, with low concentrations of SDS in the plating solutions, and (b) a small amount of large crystals with copper vacancies are formed on the substrate with high concentrations of SDS in the plating solutions.

(i.e., the growth rate of crystals). Therefore, the morphology of Cu_2O films are tunable by controlling the concentration of SDS.

In previous studies, tailoring morphology of Cu_2O crystals employing preferential adsorption of SDS on facets with high surface energy have been reported by chemical or electrochemical methods.[20,27,28,33−35] The concentrations of SDS employed in previous studies[20,27,28,33−35] were much higher than the critical micelle concentration (CMC) of SDS (8 mM in the water[33] and can be lower than 2 mM with the addition of Cu^{2+} ions[32]), such as 170[27] and 30 mM.[28,34] With a high concentration of SDS, there are sufficient SDS molecules adsorbed on the surface of Cu_2O crystals leading to a preferential growth of the facets with low surface energy. However, in this work, the morphologies of crystals are identical at the beginning of electrodeposition with the increase of SDS concentration, as shown in Figure 2. It is because that the concentrations of SDS in plating solution are 0.75−3.30 mM, which are around the CMC of SDS in the water containing Cu^{2+} ions. With such low concentrations (0.75−3.30 mM), the SDS molecules are insufficient to be adsorbed on the facets with high surface energy, and hence, the effects of SDS on the preferential growth of Cu_2O crystals with low surface energy are not significant.

3.2. Structure and Composition of Cu_2O Films. The X-ray diffraction (XRD) analyses (Figure 4) show that all Cu_2O thin films are polycrystalline cubic phase (JCPDS 65-3288) with preferentially orientation in (111) planes. The result indicates that the SDS molecules are preferentially be adsorbed on the (100) and (110) planes and then promote the growth of (111) planes. The peaks located at 2θ = 43.40 and 50.67° were

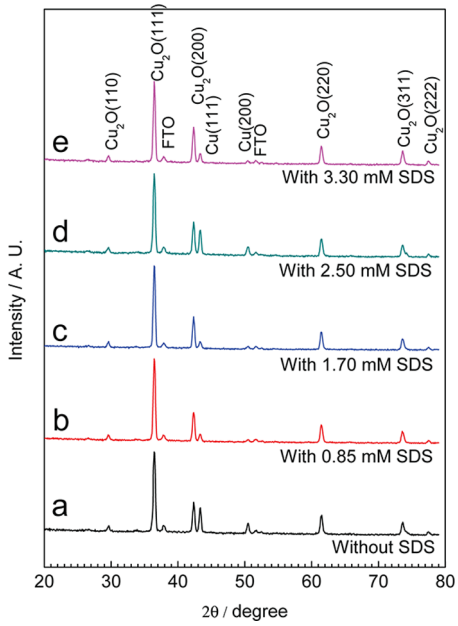

Figure 4. XRD patterns of Cu_2O thin films electrodeposited on FTO in cupric acetate solutions (pH 4.93) with different concentrations of SDS. (a) Without SDS, (b) 0.85 mM, (c) 1.70 mM, (d) 2.50 mM, and (e) 3.30 mM.

attributed to metallic copper (JCPDS 65-9026). All the XRD patterns of Cu_2O films deposited with different concentrations of SDS are identical, which indicates that the crystal structures of Cu_2O films were not affected by the change of SDS concentrations.

The metallic copper in deposited Cu_2O films comes from the reduction of Cu^{2+} or Cu_2O at −0.1 V (0.122 V_{NHE}) in the plating solution with pH 4.93 according to eqs 2 and 3. Because the overpotential for the reduction of Cu_2O to metallic copper is low (around 0.06 V), most of metallic copper in the film should come directly from the reduction of Cu^{2+} ions in the plating solution. If a higher negative deposition potential (i.e., a higher overpotential) is used, a higher content of metallic copper in Cu_2O films can be obtained.[36] The appearance of metallic copper in Cu_2O thin film was also observed in other studies.[36−39]

To character the oxidation states of Cu in Cu_2O films, the XPS spectra of both the as-deposited Cu_2O films and the bulks (i.e., the fresh Cu_2O films after the outermost surfaces were etched away) were measured, as shown in Figure 5a,b, respectively. The XPS spectra of both the as-deposited Cu_2O films and the bulk of all Cu_2O films show Cu 2p3/2 and Cu 2p1/2 at 932.4 and 952.2 eV, respectively. The primary peak located at 932.4 eV can be assigned to Cu_2O.[1,40−43] As for the as-deposited Cu_2O films, a shoulder peak located at 934.4 eV is attributed to CuO.[1,40,43] But the Cu^{2+} peak disappears totally in the bulk of Cu_2O films (Figure 5b). Therefore, the CuO only exists on the outermost surface of deposited Cu_2O films, which is attributed to the fast oxidation of Cu_2O on the film surface in air.[44]

3.3. Semiconductor Properties of Cu_2O Films. The band gap E_g of the Cu_2O films can be determined by using the relationship between the absorption coefficient α and photon energy $h\nu$,[45]

$$\alpha h\nu = A(h\nu - E_g)^{1/2} \quad (4)$$

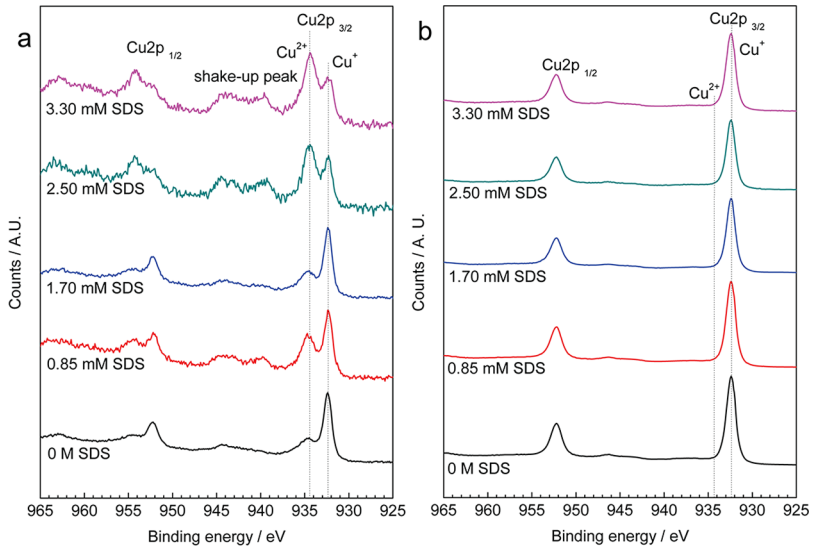

Figure 5. XPS spectra of Cu 2p for the Cu_2O films deposited in cupric acetate solutions (pH 4.93) with different SDS concentrations. (a) The as-deposited Cu_2O films, and (b) the fresh Cu_2O films after the outermost surfaces were etched away.

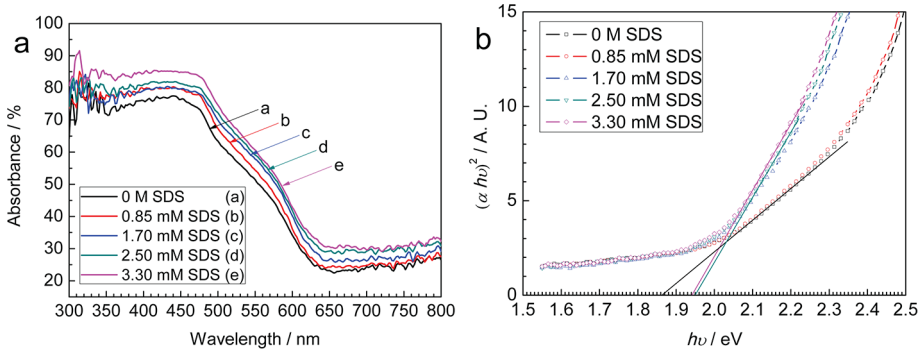

Figure 6. (a) UV−vis absorption spectra and (b) $(\alpha h\nu)^2$ vs $h\nu$ plots of the Cu_2O films electrodeposited in cupric acetate solutions with different SDS concentrations.

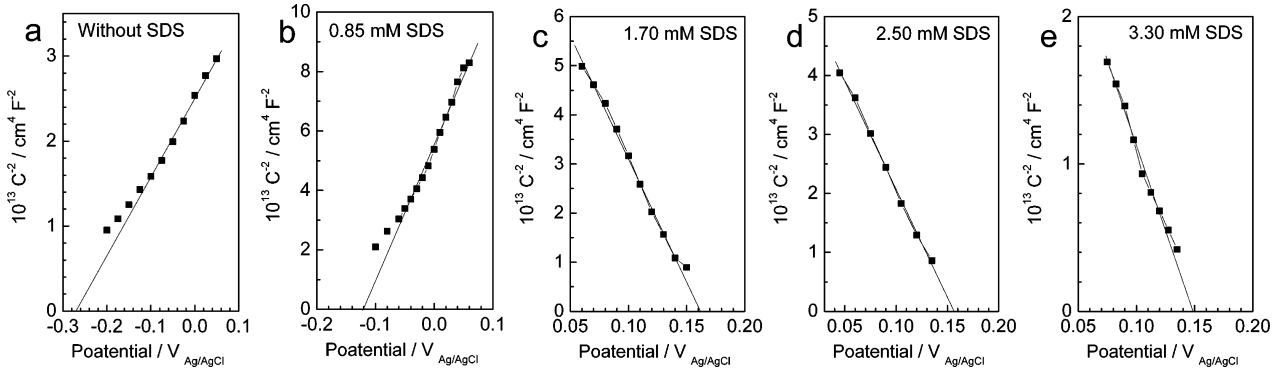

Figure 7. Mott−Schottky plots of the Cu_2O films electrodeposited in cupric acetate solutions with (a) 0 M, (b) 0.85 mM, (c) 1.70 mM, (d) 2.50 mM, and (e) 3.30 mM SDS in 3 wt % NaCl solutions.

where A is a constant; α could be estimated from the adsorption spectra according to the following equation,

$$\alpha = [\ln(1/T_{tran})]/d \quad (5)$$

where T_{tran} presents the transmittance and d is the film thickness.

Figure 6a,b shows UV−vis absorption spectra and $(\alpha h\nu)^2$ vs $h\nu$ plots of the Cu_2O films, respectively. The absorption spectra illustrate that the cutoff appears at ca. 640 nm. The band gaps of the Cu_2O films estimated from Figure 6b are ca. 1.87 eV for the films deposited with SDS concentrations lower than 0.85 mM and ca. 1.95 eV for the films deposited with SDS concentrations higher than 1.75 mM. These values are in a good agreement with literature data for Cu_2O thin films prepared by electrodeposition.[22,37,39]

The type of conductivity (i.e., n-type or p-type) of the Cu_2O films can be determined through Mott−Schottky measurements.[46] At the interface of a semiconductor film and solution,

the potential dependence of space charge layer is described by the Mott–Schottky equation:[47]

$$\frac{1}{C^2} = \frac{2}{eN_D\varepsilon\varepsilon_0}\left(E - E_{fb} - \frac{kT}{e}\right) \quad (6)$$

for an n-type semiconductor in a solution, or

$$\frac{1}{C^2} = \frac{2}{-eN_A\varepsilon\varepsilon_0}\left(E - E_{fb} - \frac{kT}{e}\right) \quad (7)$$

for a p-type semiconductor in a solution, in which C represents the capacitance of the space charge layer; N_D and N_A are the concentration of donors and acceptors, respectively; ε is the dielectric constant of the Cu_2O film and is taken as 7.6[48,49] in this case; ε_0 is the vacuum permittivity (8.85×10^{-12} F m^{-1}); e is the elementary charge (1.602×10^{-19} C); E is the electrode potential; E_{fb} is the flat band potential; k is the Boltzmann constant; and T is the absolute temperature.

Figure 7 shows the Mott–Schottky plots for Cu_2O films in 3 wt % NaCl solution. The Cu_2O films electrodeposited in plating solutions with SDS concentrations lower than 0.85 mM show n-type conductivity (Figure 7a,b) according to the linear increases of C^{-2} with the electrode potential (i.e., positive slopes in Mott–Schottky plots). However, the Cu_2O films electrodeposited in plating solutions with SDS concentrations higher than 1.70 mM show p-type conductivity (Figure 7c–e), which was indicated by the linear decreases of C^{-2} with the increase of the electrode potential (i.e., negative slopes in Mott–Schottky plots). The donor concentration of n-type Cu_2O films and the acceptor concentration of p-type Cu_2O films can be calculated from the slope of the experimental Mott–Schottky plots, and the flat band potential of the Cu_2O films in NaCl solutions can be extrapolated from $C^{-2} = 0$. The values of carrier concentrations and the flat band potentials of Cu_2O films are listed in Table 1. It can be seen that the concentration of carriers increases with the increase of SDS concentration in plating solution for both n-type and p-type Cu_2O films. For n-type Cu_2O films, the increase of donor concentration makes the Fermi level move away from the conduction band and consequently increases the flat band potential. On the contrary, for p-type Cu_2O films, the increase of acceptor concentration makes the Fermi level move away from the valence band and decreases the flat band potential.

Table 1. Density of Carriers and Flat Band Potential of Cu_2O Films in 3 wt % NaCl Solutions

SDS concentration (mM)	electrical conductivity	density of carriers		flat band potential ($V_{Ag/AgCl}$)
		N_D (cm^{-3})	N_A (cm^{-3})	
0	n-type	2.03×10^{17}		−0.263
0.85	n-type	4.06×10^{17}		−0.120
1.70	p-type		3.68×10^{17}	0.161
2.50	p-type		5.07×10^{17}	0.157
3.30	p-type		7.98×10^{17}	0.148

The mechanism of the tunable conductivity of Cu_2O films (i.e., n-type or p-type) by controlling the concentration of surfactants is illustrated in Scheme 2. The reduction of Cu^{2+} ions on FTO surface is the dominating reaction in the case that there is no SDS in plating solution. When the SDS concentrations are lower than 0.85 mM, a minute amount of SDS exists on the FTO surfaces or adsorbs on the Cu^{2+} ions in the plating solution (Scheme 2a). Therefore, plenty of Cu^{2+} ions contact the FTO surfaces, which are not covered by SDS, resulting in higher reduction rates of Cu^{2+} ions and faster growth of the crystal during the deposition. Rich oxygen vacancies or Cu^+ ions are formed in the films during such a fast reduction process, and consequently, the films show n-type conductivities, and oxygen vacancies are responsible for donor levels.[50,51] However, with the increase of SDS concentrations to 1.70 mM in plating solutions, SDS molecules occupy more area on FTO surfaces and meanwhile adsorb on more Cu^{2+} ions in the solution, which hinders the contacting of Cu^{2+} ions with FTO surfaces and results in low rates of reduction of Cu^{2+} ions (Scheme 2b). Cu vacancies are formed during the slow reduction process. Meanwhile, since Cu^+ ions in the film diffuse from the surface to the bulk, Cu vacancies become rich in the films, which results in the p-type conductivities of the films,[52,53] and Cu vacancies are responsible for acceptor levels.

The photocurrent measurements of the electrodeposited Cu_2O films are performed at the open circuit potential (−0.05 V) in 3 wt % NaCl solutions. Figure 8 shows the photocurrent response of each Cu_2O film. For n-type Cu_2O electrodes (Figure 8a,b), anodic photocurrents appear due to the oxidation reaction resulting from the photogenerated holes. The decrease of photocurrents with the increase of SDS concentration is attributed to the decrease of band bending (i.e., the difference between the electrode potential and the flat band potential), even though the carrier concentration increases. However, for p-type Cu_2O electrodes (Figure 8c–e), cathodic photocurrents appear owing to the reduction reaction resulting from the photogenerated electrons. Combining the effect of carrier concentrations and band bending, the Cu_2O film electrodeposited with 2.50 mM SDS shows the highest photocurrent. It should be noted that the spike and overshoot (Figure 8c–e) of photocurrents are gradually eliminated with the increase of SDS concentration during electrodepositing Cu_2O, indicating the decrease of the recombination of photogenerated electron–hole pairs.[54]

4. CONCLUSIONS

The present work shows a facile way to tune the morphology and electrical conductivity of Cu_2O films in one pot by controlling the concentration of surfactants in the plating solution. For Cu_2O films electrodeposited in cupric acetate solution (pH 4.93), the average size of crystals increases and the amount of crystals decreases with the increase of SDS concentration in the plating solutions. The Cu_2O crystals show lateral preferential growth on the FTO glass, and all the Cu_2O thin films are polycrystalline cubic phase with preferentially orientation in (111) planes. The concentration of SDS affects the crystal growth rate but not the crystal structure. The SDS in the plating solutions also affects the conductivity of Cu_2O films by means of controlling the reduction rate of cupric ions. When the SDS concentrations are lower than 0.85 mM in the plating solution, the electrodeposited Cu_2O films show n-type conductivities due to the formation of oxygen vacancies. With the increase of SDS concentration in the plating solutions, the donor concentration increases, and the flat band potential moves to the positive direction. The band gap for the electrodeposited n-type Cu_2O is about 1.87 eV, and the photocurrent decreases with the addition of SDS. When the SDS concentrations are higher than 1.70 mM in the plating solution, the electrodeposited Cu_2O films show p-type conductivities owing to the formation of copper vacancies.

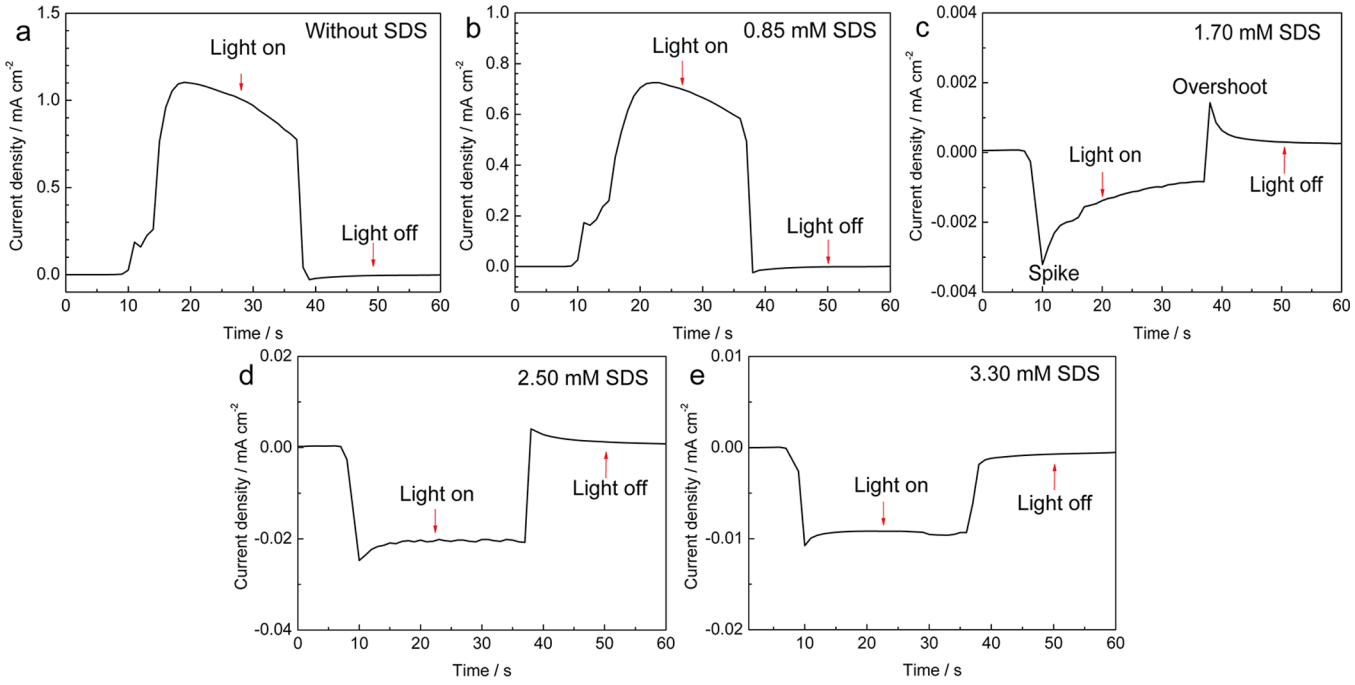

Figure 8. Photocurrent responses of Cu_2O films electrodeposited in plating solutions with varying SDS concentrations of (a) 0 M, (b) 0.85 mM, (c) 1.70 mM, (d) 2.50 mM, and (e) 3.30 mM at OCP.

With the increase of SDS concentration in the plating solutions, the acceptor concentration increases, and the flat band potential moves to the negative direction. The band gap for the electrodeposited p-type Cu_2O is about 1.95 eV, and the highest photocurrent appears when the SDS concentration is 2.50 mM. The method shown in this work can conveniently tune the conductivity of Cu_2O films in one pot and therefore paves a promising way for the building of Cu_2O homojunction electrodes in the future.

■ ASSOCIATED CONTENT

Supporting Information

Polarization curves of FTO glass in plating solutions with different concentrations of SDS, detailed SEM images for illustrating the morphology evolution of Cu_2O crystal growth during electrodeposition, and electrochemical impedance spectra (EIS) analyses of FTO glass and Cu_2O films in water containing different concentrations of SDS. This material is available free of charge via the Internet at http://pubs.acs.org.

■ AUTHOR INFORMATION

Corresponding Authors

*E-mail: yingyang@nwu.edu.cn.
*E-mail: wxu1@stevens.edu.

Notes

The authors declare no competing financial interest.

■ ACKNOWLEDGMENTS

Cu_2O films fabrication and PEC measurements were supported by the National Science Foundation of China (No. 51302216) and the Open Fund of the State Key Laboratory of Multiphase Flow in Power Engineering of China. SEM and XPS characterizations were supported by the Natural Science Basic Research Plan in Shaanxi Province of China (No. 2013JQ2007) and the Scientific Research Program Funded by Shaanxi Provincial Education Department (No.14JK1765).

■ REFERENCES

(1) Zhang, Z.; Dua, R.; Zhang, L.; Zhu, H.; Zhang, H.; Wang, P. Carbon-Layer-Protected Cuprous Oxide Nanowire Arrays for Efficient Water Reduction. *ACS Nano* **2013**, *7*, 1709−1717.

(2) Zhang, X.; Yu, S.; Cao, Y.; Chen, L.; Zhao, T.; Yang, F. Cu_2O-Coated Polystyrene Microsphere Materials with Enhanced Photo- and Photoelectro-Catalytic Activity. *J. Solid State Electrochem.* **2013**, *17*, 1429−1434.

(3) Huang, Q.; Kang, F.; Liu, H.; Li, Q.; Xiao, X. Highly Aligned Cu_2O/CuO/TiO_2 Core/Shell Nanowire Arrays as Photocathodes for Water Photoelectrolysis. *J. Mater. Chem. A* **2013**, *1*, 2418−2425.

(4) Paracchino, A.; Laporte, V.; Sivula, K.; Grätzel, M.; Thimsen, E. Highly Active Oxide Photocathode for Photoelectrochemical Water Reduction. *Nat. Mater.* **2011**, *10*, 456−461.

(5) Dong, C.; Zhong, M.; Huang, T.; Ma, M.; Wortmann, D.; Brajdic, M.; Kelbassa, I. Photodegradation of Methyl Orange under Visible Light by Micro-Nano Hierarchical Cu_2O Structure Fabricated by Hybrid Laser Processing and Chemical Dealloying. *ACS Appl. Mater. Interfaces* **2014**, *3*, 4332−4338.

(6) Liu, L.; Yang, W.; Li, Q.; Gao, S.; Shang, J. K. Synthesis of Cu_2O Nanospheres Decorated with TiO_2 Nanoislands, Their Enhanced Photoactivity and Stability under Visible Light Illumination, and Their Post-Illumination Catalytic Memory. *ACS Appl. Mater. Interfaces* **2014**, *6*, 5629−5639.

(7) Gershon, T.; Musselman, K. P.; Marin, A.; Friend, R. H.; MacManus-Driscoll, J. L. Thin-Film ZnO/Cu_2O Solar Cells Incorporating an Organic Buffer Layer. *Sol. Energy Mater. Sol. Cells* **2011**, *96*, 148−154.

(8) Duan, Z.; Pereira, N.; Lu, Y.; Du Pasquier, A. Gel Probe Photocurrent Measurement of Cuprous Oxide Films. *Sol. Energy Mater. Sol. Cells* **2010**, *94*, 1741−1746.

(9) Cao, D.; Wang, C.; Zheng, F.; Dong, W.; Fang, L.; Shen, M. High-Efficiency Ferroelectric-Film Solar Cells with an n-Type Cu_2O Cathode Buffer Layer. *Nano Lett.* **2012**, *12*, 2803−2809.

(10) Han, K.; Tao, M. Electrochemically Deposited p-n Homojunction Cuprous Oxide Solar Cells. *Sol. Energy Mater. Sol. Cells* **2009**, *93*, 153−157.

(11) Rajeshwar, K.; de Tacconi, N. R.; Ghadimkhani, G.; Chanmanee, W.; Janáky, C. Tailoring Copper Oxide Semiconductor

Nanorod Arrays for Photoelectrochemical Reduction of Carbon Dioxide to Methanol. *ChemPhysChem* **2013**, *14*, 2251−2259.
(12) Qiao, J.; Jiang, P.; Liu, J.; Zhang, J. Formation of Cu Nanostructured Electrode Surfaces by an Annealing-Electroreduction Procedure to Achieve High-Efficiency CO_2 Electroreduction. *Electrochem. Commun.* **2014**, *38*, 8−11.
(13) Zhai, Q.; Xie, S.; Fan, W.; Zhang, Q.; Wang, Y.; Deng, W.; Wang, Y. Photocatalytic Conversion of Carbon Dioxide with Water into Methane: Platinum and Copper(I) Oxide Co-Catalysts with a Core−Shell Structure. *Angew. Chem., Int. Ed.* **2013**, *52*, 5776−5779.
(14) Ghadimkhani, G.; de Tacconi, N. R.; Chanmanee, W.; Janaky, C.; Rajeshwar, K. Efficient Solar Photoelectrosynthesis of Methanol from Carbon Dioxide Using Hybrid CuO−Cu_2O Semiconductor Nanorod Arrays. *Chem. Commun.* **2013**, *49*, 1297−1299.
(15) Grace, A. N.; Choi, S. Y.; Vinoba, M.; Bhagiyalakshmi, M.; Chu, D. H.; Yoon, Y.; Nam, S. C.; Jeong, S. K. Electrochemical Reduction of Carbon Dioxide at Low Overpotential on a Polyaniline/Cu_2O Nanocomposite Based Electrode. *Appl. Energy* **2014**, *120*, 85−94.
(16) Scanlon, D. O.; Morgan, B. J.; Watson, G. W.; Walsh, A. Acceptor Levels in p-Type Cu_2O: Rationalizing Theory and Experiment. *Phys. Rev. Lett.* **2009**, *103*, 096405.
(17) Zouaghi, M.; Prevot, B.; Carabatos, C.; Sieskind, M. Near Infrared Optical and Photoelectric Properties of Cu_2O. III. Interpretation of Experimental Results. *Phys. Status Solidi A* **1972**, *11*, 449−460.
(18) Wijesundera, R. P.; Hidaka, M.; Koga, K.; Sakai, M.; Siripala, W.; Choi, J.-Y.; Sung, N. E. Effects of Annealing on the Properties and Structure of Electrodeposited Semiconducting Cu−O Thin Films. *Phys. Status Solidi B* **2007**, *244*, 4629−4642.
(19) Ci, J.-W.; Tu, W.-C.; Uen, W.-Y.; Lan, S.-M.; Zeng, J.-X.; Yang, T.-N.; Shen, C.-C.; Jhao, J.-C. Chlorine-Doped n-Type Cuprous Oxide Films Fabricated by Chemical Bath Deposition. *J. Electrochem. Soc.* **2014**, *161*, D321−D326.
(20) McShane, C. M.; Choi, K.-S. Photocurrent Enhancement of n-Type Cu_2O Electrodes Achieved by Controlling Dendritic Branching Growth. *J. Am. Chem. Soc.* **2009**, *131*, 2561−2569.
(21) Tsui, L.-K.; Zangari, G. The Influence of Morphology of Electrodeposited Cu_2O and Fe_2O_3 on the Conversion Efficiency of TiO_2 Nanotube Photoelectrochemical Solar Cells. *Electrochim. Acta* **2013**, *100*, 220−225.
(22) Zhao, W.; Fu, W.; Yang, H.; Tian, C.; Li, M.; Li, Y.; Zhang, L.; Sui, Y.; Zhou, X.; Chen, H.; Zou, G. Electrodeposition of Cu_2O Films and Their Photoelectrochemical Properties. *CrystEngComm* **2011**, *13*, 2871−2877.
(23) Golden, T. D.; Shumsky, M. G.; Zhou, Y.; VanderWerf, R. A.; Van Leeuwen, R. A.; Switzer, J. A. Electrochemical Deposition of Copper(I) Oxide Films. *Chem. Mater.* **1996**, *8*, 2499−2504.
(24) de Jongh, P. E.; Vanmaekelbergh, D.; Kelly, J. J. Cu_2O: Electrodeposition and Characterization. *Chem. Mater.* **1999**, *11*, 3512−3517.
(25) Jiang, T.; Xie, T.; Yang, W.; Chen, L.; Fan, H.; Wang, D. Photoelectrochemical and Photovoltaic Properties of p-n Cu_2O Homojunction Films and Their Photocatalytic Performance. *J. Phys. Chem. C* **2013**, *117*, 4619−4624.
(26) Liau, L. C.-K.; Lin, Y.-C.; Peng, Y.-J. Fabrication Pathways of p-n Cu_2O Homojunction Films by Electrochemical Deposition Processing. *J. Phys. Chem. C* **2013**, *117*, 26426−26431.
(27) Siegfried, M. J.; Choi, K. S. Electrochemical Crystallization of Cuprous Oxide with Systematic Shape Evolution. *Adv. Mater.* **2004**, *16*, 1743−1746.
(28) Wang, X.; Liu, C.; Zheng, B.; Jiang, Y.; Zhang, L.; Xie, Z.; Zheng, L. Controlled Synthesis of Concave Cu_2O Microcrystals Enclosed by {hhl} High-Index Facets and Enhanced Catalytic Activity. *J. Mater. Chem. A* **2013**, *1*, 282−287.
(29) Pourbaix, M. *Atlas of Electrochemical Equilibria in Aqueous Solutions*. National Association of Corrosion Engineers: Houston, 1974.
(30) Han, X.; Han, K.; Tao, M. n-Type Cu_2O by Electrochemical Doping with Cl. *Electrochem. Solid-State Lett.* **2009**, *12*, H89−H91.
(31) Zheng, Z.; Huang, B.; Wang, Z.; Guo, M.; Qin, X.; Zhang, X.; Wang, P.; Dai, Y. Crystal Faces of Cu_2O and Their Stabilities in Photocatalytic Reactions. *J. Phys. Chem. C* **2009**, *113*, 14448−14453.
(32) Su, S.-G.; Chen, Y. L.; Mou, C. Y. Micelle-Counterion Interaction, I. Critical Micelle Concentrations of SDS under the Influence of Copper Counterion. *J. Chin. Chem. Soc.* **1985**, *32*, 5−10.
(33) Naskar, B.; Dey, A.; Moulik, S. Counter-Ion Effect on Micellization of Ionic Surfactants: A Comprehensive Understanding with Two Representatives, Sodium Dodecyl Sulfate (SDS) and Dodecyltrimethylammonium Bromide (DTAB). *J. Surfactants Deterg.* **2013**, *16*, 785−794.
(34) Ho, J.-Y.; Huang, M. H. Synthesis of Submicrometer-Sized Cu_2O Crystals with Morphological Evolution from Cubic to Hexapod Structures and Their Comparative Photocatalytic Activity. *J. Phys. Chem. C* **2009**, *113*, 14159−14164.
(35) Kuo, C.-H.; Huang, M. H. Facile Synthesis of Cu_2O Nanocrystals with Systematic Shape Evolution from Cubic to Octahedral Structures. *J. Phys. Chem. C* **2008**, *112*, 18355−18360.
(36) Wijesundera, R. P.; Hidaka, M.; Koga, K.; Sakai, M.; Siripala, W. Growth and Characterisation of Potentiostatically Electrodeposited Cu_2O and Cu Thin Films. *Thin Solid Films* **2006**, *500*, 241−246.
(37) Yu, X.; Li, X.; Zheng, G.; Wei, Y.; Zhang, A.; Yao, B. Preparation and Properties of KCl-Doped Cu_2O Thin Film by Electrodeposition. *Appl. Surf. Sci.* **2013**, *270*, 340−345.
(38) Mizuno, K.; Izaki, M.; Murase, K.; Shinagawa, T.; Chigane, M.; Inaba, M.; Tasaka, A.; Awakura, Y. Structural and Electrical Characterizations of Electrodeposited p-Type Semiconductor Cu_2O Films. *J. Electrochem. Soc.* **2005**, *152*, C179−C182.
(39) Paracchino, A.; Brauer, J. C.; Moser, J.-E.; Thimsen, E.; Graetzel, M. Synthesis and Characterization of High-Photoactivity Electrodeposited Cu_2O Solar Absorber by Photoelectrochemistry and Ultrafast Spectroscopy. *J. Phys. Chem. C* **2012**, *116*, 7341−7350.
(40) Zhu, C.; Osherov, A.; Panzer, M. J. Surface Chemistry of Electrodeposited Cu_2O Films Studied by XPS. *Electrochim. Acta* **2013**, *111*, 771−778.
(41) Yin, M.; Wu, C.-K.; Lou, Y.; Burda, C.; Koberstein, J. T.; Zhu, Y.; O'Brien, S. Copper Oxide Nanocrystals. *J. Am. Chem. Soc.* **2005**, *127*, 9506−9511.
(42) Teo, J. J.; Chang, Y.; Zeng, H. C. Fabrications of Hollow Nanocubes of Cu_2O and Cu via Reductive Self-Assembly of CuO Nanocrystals. *Langmuir* **2006**, *22*, 7369−7377.
(43) Barreca, D.; Gasparotto, A.; Tondello, E. CVD Cu_2O and CuO Nanosystems Characterized by XPS. *Surf. Sci. Spectra* **2007**, *14*, 41−51.
(44) Ram, S.; Mitra, C. Formation of Stable Cu_2O Nanocrystals in a New Orthorhombic Crystal Structure. *Mater. Sci. Eng., A* **2001**, *304*−*306*, 805−809.
(45) Peter, L. M.; Tributsch, H. In *Nanostructured and Photoelectrochemical Systems for Solar Photon Conversion*; Archer, M. D., Nozik, A. J., Eds.; Imperial College Press: London, 2008; Chapter 12, pp 675−736.
(46) Nozik, A. J.; Memming, R. Physical Chemistry of Semiconductor−Liquid Interfaces. *J. Phys. Chem.* **1996**, *100*, 13061−13078.
(47) Bott, A. W. Electrochemistry of Semiconductors. *Curr. Sep.* **1998**, *17*, 87−91.
(48) Zhang, Z.; Wang, P. Highly Stable Copper Oxide Composite as an Effective Photocathode for Water Splitting via a Facile Electrochemical Synthesis Strategy. *J. Mater. Chem.* **2012**, *22*, 2456−2464.
(49) Hsu, Y.-K.; Yu, C.-H.; Chen, Y.-C.; Lin, Y.-G. Synthesis of Novel Cu_2O Micro/Nanostructural Photocathode for Solar Water Splitting. *Electrochim. Acta* **2013**, *105*, 62−68.
(50) Siripala, W.; Jayakody, J. R. P. Observation of n-Type Photoconductivity in Electrodeposited Copper Oxide Film Electrodes in a Photoelectrochemical Cell. *Sol. Energy Mater.* **1986**, *14*, 23−27.
(51) Garuthara, R.; Siripala, W. Photoluminescence Characterization of Polycrystalline n-Type Cu_2O Films. *J. Lumin.* **2006**, *121*, 173−178.
(52) Raebiger, H.; Lany, S.; Zunger, A. Origins of the p-Type Nature and Cation Deficiency in Cu_2O and Related Materials. *Phys. Rev. B* **2007**, *76*, 045209.

(53) Nolan, M.; Elliott, S. D. The p-Type Conduction Mechanism in Cu_2O: A First Principles Study. *Phys. Chem. Chem. Phys.* **2006**, *8*, 5350−5358.
(54) Peter, L. Energetics and Kinetics of Light-Driven Oxygen Evolution at Semiconductor Electrodes: The Example of Hematite. *J. Solid State Electrochem.* **2013**, *17*, 315−326.

NOTE ADDED AFTER ASAP PUBLICATION

This paper was published on the Web on December 10, 2014, with a minor error in eq 3. The corrected version was reposted on December 11, 2014. After the paper was posted on December 11, 2014, additional corrections were made to eqs 6 and 7. The corrected version was reposted on December 12, 2014.